Neural Probes with Integrated Temperature Sensors for Monitoring Retina and Brain Implantation and Stimulation

Jiaqi Wang, Hui Xie, Tsing Chung, Leanne Lai Hang Chan, *Member, IEEE*, and Stella W. Pang, *Fellow, IEEE*

***Abstract*— Gold (Au) resistive temperature sensors were integrated on flexible polyimide-based neural probes to monitor temperature changes during neural probe implantation and stimulation. Temperature changes were measured as neural probes were implanted to infer the positions of the neural probes, and as the retina or the deep brain region was stimulated electrically. The temperature sensor consisted of a serpentine Au resistor and surrounded by four Au electrodes with 200 and 400 μm diameter (dia.). The Au temperature sensors had temperature coefficient of 0.32%, and they were biocompatible and small in size. *In vivo* measurements of temperature changes during implantation and stimulation were carried out in the retina and deep brain region in rats. The desired implantation position was reached when temperature measured by the sensor increased to the calibrated level and became stable. There was no temperature increase when low level stimulation current of 8 and 13 μA each for the two 200- and 400-μm-dia. electrodes, respectively, were applied. When higher level stimulation current of 100 and 200 μA each were applied to the two 200- and 400- μm-dia. electrodes, respectively, maximum temperature increases of 1.2 °C in retina and 1 °C in deep brain region were found.**

***Index Terms*— Flexible neural probe, integrated temperature sensor, temperature increase, probe position, stimulation.**

I. Introduction

TISSUE temperature increase induced by electrical stimulation should be limited because abnormal body temperature affects many biological reactions [1]–[5]. It has been reported that tissue temperature could increase during electrical stimulation through electrodes on neural probes [6], [7]. For future generation of neural probes with more than 1000 electrodes, temperature rise due to stimulation by a large number of electrodes could be significant [8]. Therefore, tissue temperature during electrical stimulation should be monitored, as temperature increase should be kept to <2 °C to avoid physiological abnormality in retina [9]. Even though self-regulated tissue temperature related to immune or metabolic responses could help to prevent temperature increase due to blood perfusion or induced tears [10], [11], any temperature increase caused by electrical stimulation should be kept to a minimum to avoid tissue damage. In addition to neural stimulation, temperature increases were also reported due to laser [12], RF source [13], and electromagnetic wave irradiation [14]. Thus, development of an *in vivo* temperature sensor integrated on a neural probe for temperature monitoring is necessary to prevent stimulation induced thermal damage to the tissue.

A number of methods have been developed to obtain the tissue temperature around neural probes. Noninvasive methods to monitor neural probe temperature include infrared camera [15] and optoacoustic detection [16], [17]. These methods did not require implantation surgery of temperature sensors in the body. However, human body could block the infrared or optoacoustic wave. Invasive temperature sensors such as thermocouple probe were implanted in the body or tissue to monitor temperature changes [18], [19]. These temperature sensors have to be biocompatible since they are implanted inside the body. Commercial thermal resistors and thermocouples [20], [21] were inserted next to neural probes for temperature measurements. These approaches have the disadvantages of requiring additional surgery and large in size that could generate damage to the tissue. Simulations using finite element method (FEM) were also developed to study temperature distribution around the electrodes of neural probes [22]–[24]. Results from stimulation need to be verified by *in vivo* temperature measurements.

As neural probe is inserted into the retina or deep brain region, probe temperature initially increases from air temperature to a stable temperature of the tissue. For probe implantation into the retina or deep brain region, visual inspection of the probe position is difficult and stereotactic imaging may be limited. It will be useful to have an alternative way to monitor the position of the inserted neural probe to determine whether the probe has reached the desired location. Due to heat exchange with air, temperature variations from the

Manuscript received August 6, 2015; revised December 3, 2015 and July 23, 2016; accepted November 10, 2016. Date of publication March 2, 2017; date of current version September 2, 2017. This work was supported in part by the Centre for Biosystems, Neuroscience, and Nanotechnology and City University of Hong Kong under Grant 9360148 and Grant 9380062, in part by the University Grants Council of Hong Kong under Grant GRF 120413, Grant 123412, Grant 11210814, Grant 11247716, and Grant C1013-15G, and in part by the Hong Kong Scholars Program. *(Corresponding author: Stella W. Pang.)*

J. Wang is with the Department of Electronic Engineering and the Centre for Biosystems, Neuroscience and Nanotechnology, City University of Hong Kong, Hong Kong, and also with the College of Electronic Science and Technology, Dalian University of Technology, Dalian, China (e-mail: jiaqwang@cityu.edu.hk).

H. Xie, T. Chung, L. L. H. Chan, and S. W. Pang are with the Department of Electronic Engineering and the Centre for Biosystems, Neuroscience and Nanotechnology, City University of Hong Kong, Hong Kong, (e-mail: huixie@cityu.edu.hk; janjanetchung@gmail.com; lhlchan@cityu.edu.hk; pang@cityu.edu.hk).

Digital Object Identifier 10.1109/TNSRE.2016.2634584

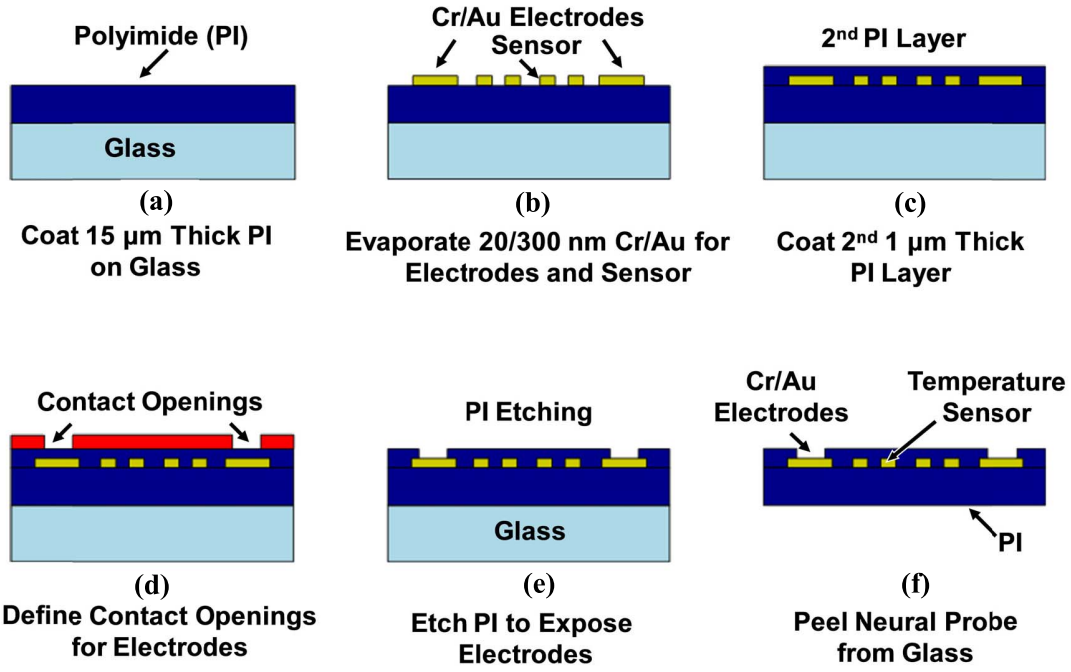

Fig. 1. Fabrication process for neural probe with integrated temperature sensor. (a) 15 μm thick PI was coated on glass substrate. (b) 20/300 nm Cr/Au was evaporated and patterned for electrodes and temperature sensor. (c) Second PI layer was coated on surface. (d) Contact openings were defined for electrodes. (e) PI was etched to expose electrodes by reactive ion etching (RIE). (f) Neural probe was peeled off from glass substrate.

surface to the core of tissue is expected, as indicated in the results shown in this paper. Our results agree with previous publication [25] which showed increase of temperature from the cooler peripheral areas to a warmer brain core. Moreover, for chronic neural recording or stimulation using the neural probe in the brain, the probe position may shift or move to the surface, but it cannot be checked visually because the incision was covered. In this case, the temperature sensor could record temperature changes related to movement of the probe when it is out of its designated position.

In this paper, gold (Au) resistive temperature sensors were integrated on neural probes for neural signal recording and stimulation. The integrated temperature sensors were small in size and utilized the same Au metal for the electrodes and the resistors for the sensors. They were placed in close proximity to the electrodes on the neural probes and could be used to precisely monitor temperature distribution in the tissue. *In vivo* measurements of neural probes with integrated temperature sensors were carried out by implanting the probes into the retina in the eye and deep brain region. Temperature changes during implantation and stimulation were monitored. The results showed that the Au integrated temperature sensors could monitor the temperature rise under large stimulation current.

II. Methods

A. Fabrication Process for Neural Probes and Temperature Sensors

The neural probes and the integrated temperature sensors were fabricated with polyimide (PI) (ZKPI Series, POME Sci-tech, China) as the substrate to make it flexible to avoid tissue damage and to provide better contact with the retina [26]–[28]. Au was used as the material for the electrodes and the temperature sensor. Figure 1 shows the schematics of the fabrication process. A 15 μm thick PI layer was coated on glass as the substrate for the neural probe, and cured gradually from 80 to 280 °C, as shown in figure 1(a). After cooling down, the PI layer was treated by an O_2 plasma (20 sccm O_2, 55 W RF power, 80 mTorr, and 3 min) to provide better adhesion with the electrodes [29]. 20/300 nm Cr/Au layer was evaporated on the PI substrate and patterned to form the electrodes and temperature sensors using optical lithography. Figure 1(b) shows Cr/Au layer was wet etched using the patterned photoresist as an etch mask. A second layer of 1 μm thick PI layer was coated on the top of the electrodes and cured gradually from 80 to 280 °C, as shown in figure 1(c). A 4 μm thick AZ6130 photoresist was coated and patterned as the etch mask for opening the contacts to the electrodes and bonding pads, as shown in figure 1(d). The PI was etched by the reactive ion etching (RIE) in 60/30 sccm CF_4/O_2, 90 W RF power, 20 mTorr, and 25 min to expose the electrodes and bonding pads, while still covering the temperature sensor with 1 μm thick PI layer, as shown in figure 1(e). Figure 1(f) shows the neural probe after being peeled off from the glass substrate. The neural probes were attached and bonded to the printed circuit boards (PCB) with connectors (A79016-001, Omnetics Connector Corporation, USA) by a ball bonder machine (YT2103, Shenzhen Yu Tong Electronic Device Company, China), as shown in figure 2(a).

The neural probe was 2.5 cm long and 0.8 mm wide. It consisted of two 200 μm and two 400 μm diameter (dia.) electrodes, which were similar to the electrode sizes used in the retinal prostheses development. The electrode sizes for the

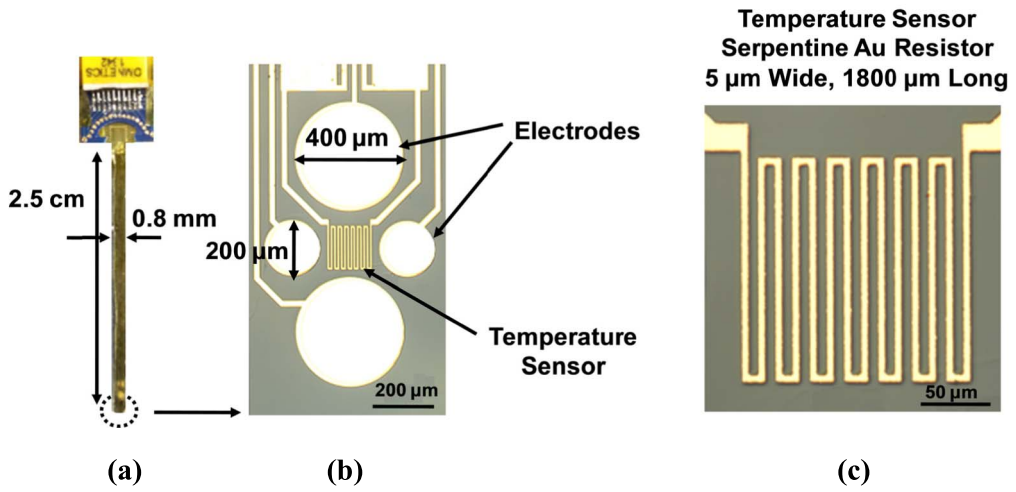

Fig. 2. Neural probe with electrodes integrated with temperature sensor. (a) Neural probe in PI substrate which was 2.5 cm long, 0.8 mm wide and 16 μm thick. (b) 200 and 400 μm dia. electrodes and temperature sensor at tip of neural probe. (c) Temperature sensor with 5 μm wide and 1800 μm long serpentine Au wires.

first generation in retinal prosthesis were 260 and 520 μm while electrode size of 200 μm was used for the second generation [30], [31]. Temperature sensor was placed in the center of the 4 electrodes and consisted of serpentine Au resistor with 5 μm wide and 1800 μm long wires, as shown in figures 2(b) and (c). Unlike the electrodes that were exposed to the tissue, the temperature sensors were covered by an insulating layer consisting of 1 μm thick PI film. Temperature sensors were calibrated in temperature-controlled water bath and the characteristics of the electrodes were tested in 0.1 M Phosphate buffered saline (PBS) solution.

B. Experimental Setup for in vivo Measurements

Adult Long-Evans (LE) rats were used for all *in vivo* measurements. They were obtained from the laboratory animal services center of the Chinese University of Hong Kong and housed with a 12 h light/dark cycle and with food and water available ad libitum. All experimental procedures were approved by the Animal Subjects Ethics Sub-Committee of City University of Hong Kong.

Rats were anesthetized using a combination solution of ketamine (70 mg/kg, Alfasan, Holland, i.p.) and xylazine (7 mg/kg, Alfasan, Holland, i.p.) by 2:1 and maintained with an anaesthesia machine (SurgiVet, Smiths Medical PM, USA) by isoflurane throughout the stereotaxic surgery and *in vivo* tests. The body temperature was monitored and kept within 35.8-37.5 °C by a heating pad (TP702, Gaymar Industries, USA). The room temperature and humidity of lab were 22 °C and 70%, respectively.

For *in vivo* testing of neural probe in retina, rats were mounted in a stereotaxic device, and two drops of tropicamide (Mydrin-P, Santen Pharmaceutical, Japan) were used to dilate the pupil and eye gel (Lubrithal, Dechra Veterinary Products A/S, Denmark) was applied from time to time throughout the experiment to maintain the moisture and clarity of the stimulated eye. A small incision was made in the upper sclera near the limbus of the eye for neural probe implantation. The neural probe was inserted through the incision into the natural gap between the lens and the retina, with an angle cling to the surface of the sclera to avoid penetrating through the lens while reaching the vitreous space of the retina. Figure 3(a) shows a neural probe implanted into the retina of an eye. The neural probe should be flexible enough to have a successful implantation into the eye and contact well with the retina.

After finishing the *in vivo* testing of neural probes in the retina, a craniotomy was performed at the occipital lobe (2.5-5.5 mm medial to lateral and 1.5-4.5 mm posterior to bregma) to access the deep brain region. The neural probe was implanted into the deep brain region at a depth up to 3 mm from the dura mater above the cortex for *in vivo* measurements. Figure 3(b) shows a neural probe implanted into the deep brain region. As shown in the figure, the 16 μm thick neural probe was attached to a 100 μm thick PI film to increase the stiffness for probe insertion. Even with the PI backing film, these neural probes were more flexible compared to silicon-based neural probes and they provided better contact with the tissue. The ground of the testing equipment was connected to the rat to ensure a uniform ground during the tests.

Different waveforms of stimulation pulses were applied for *in vivo* testing [32]–[34]. Stimulation currents were supplied by a channel stimulus generator (STG-4004, MCS GmbH, Germany). It consisted of four output channels and each channel was connected to an electrode on the neural probe. The stimulation current of each channel could be assigned independently. Charge balanced biphasic pulses were used for neural stimulation as shown in figure 3(c) and two levels of stimulation current were applied. Under the safe current limit, the stimulation current was 8 μA each for the two 200 μm dia. electrodes and 13 μA each for the two 400 μm dia. electrodes. For future generation of retinal neural probes, large number of electrodes with stimulation current beyond the safe current limit could be needed. Previous work showed the use of stimulation current up to 500 μA for 200 μm dia. electrodes and 1500 μA for 400 μm dia. electrodes [33]. In our experiment, 100 and 200 μA were chosen as stimulation currents for the 200 and 400 μm dia. electrodes,

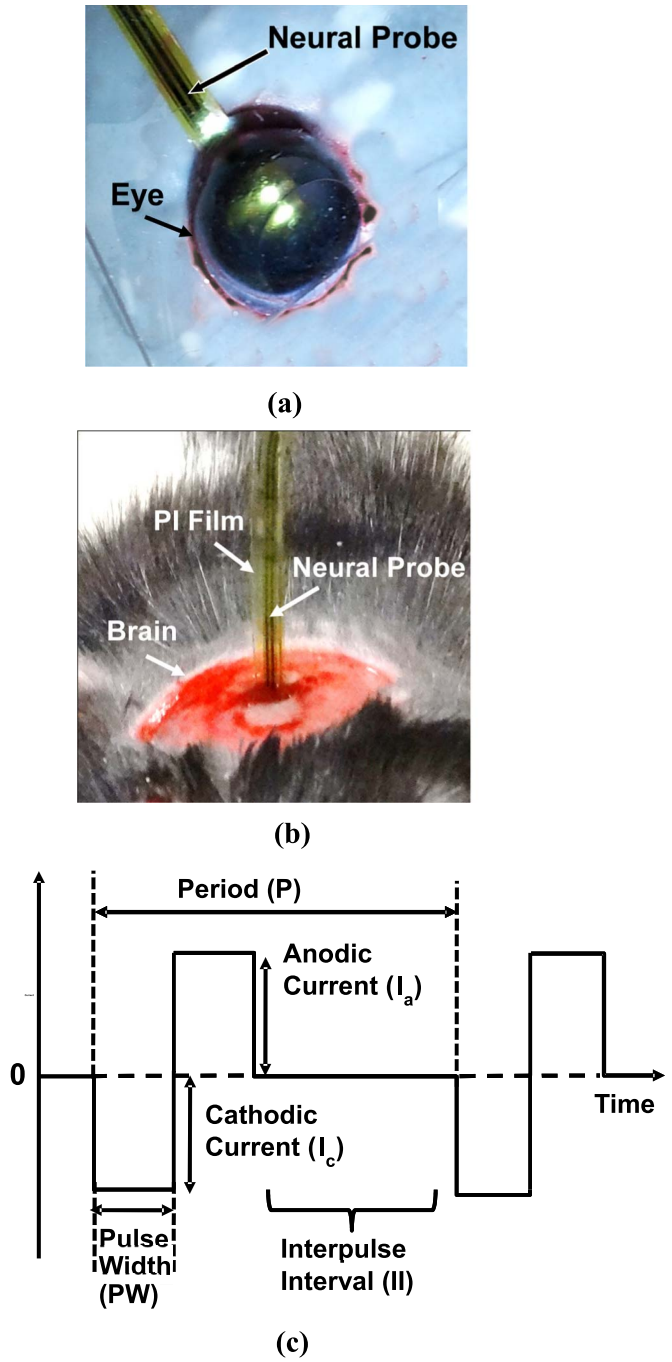

Fig. 3. Implantation of neural probe and waveform of stimulation current. (a) Implantation of neural probe in retina of eye. (b) Implantation of neural probe in deep brain region. (c) Charge balanced biphasic pulses for stimulation.

respectively, to minimize damage to the electrodes. The stimulation waveform consisted of 1 ms pulse width (PW), 20 ms period (P), 18 ms interpulse interval (II), and equal amplitude of anodic and cathodic current set to the desired stimulation current magnitude. Stimulation current was applied to the four electrodes simultaneously.

Six rats were used for the *in vivo* experiments. The data obtained from the retinal implantation was obtained from 9 different eyes of 6 rats using 9 different neural probes. The data obtained from the brain implantation was obtained from 3 different brains with 3 different neural probes. To avoid complications from previous neural probe implantation, a fresh neural probe was used for each experiment. Stimulation experiments were carried out in 30 min time intervals, including a 10 min period for stimulation and a 10 min period for resting in between stimulations. Typically each rat could last for 4 to 6 h while it was under anesthesia.

III. Results

A. Calibration of Temperature Sensors

The temperature sensors at the tips of the neural probes were calibrated in a temperature controlled water bath (TW2, JULABO Gmbh, Germany) with temperature varying from 18 to 42 °C. The temperature of the water bath was measured in close proximity to the neural probe using a PT100 temperature sensor (CRZ-2005-100-A-1, Hayashi denko, Japan) which had an accuracy of ±0.15 °C. The resistance of the temperature sensors was recorded as a function of temperature by measuring the voltage across the Au resistor as 1 mA DC current was applied. Since a DC current was needed for the temperature measurements, the self-heating effect of the Au resistor was investigated. The measured temperature and voltage across the sensors were shown in figures 4(a) and 4(b). As shown in figure 4(a) at a base temperature of 21 °C, with DC current varying from 0.2 to 3.5 mA, the self-induced temperature increase could be up to 4.2 °C. The corresponding voltage increase across the temperature sensor is shown on the right hand side axis of the plot. However, since only 1 mA DC current was used for the Au resistive temperature sensor, the temperature increase was <0.05 °C and it was a negligible self-heating effect.

As shown in figure 4(b), the resistance of the Au temperature sensors changed with temperature according to the following equation:

$$R_t = R_o[1 + \alpha(T - T_o)] \quad (1)$$

where R_t and R_o were the resistance of the temperature sensing element at the operational temperature T and reference temperature T_o, respectively, and α was the temperature coefficient of resistance (TCR). The resistance, R_o, was measured to be 185.6 Ω at 18 °C as the output voltage was 185.6 mV at 1 mA input current. At higher temperature of 41 °C, the measured voltage was 198.9 mV with the corresponding temperature sensor resistance of 198.9 Ω. The Au temperature sensors showed a good linearity and the TCR of the sensor was 0.32%. It was comparable to previously reported Au and Pt temperature sensors with TCR ranging from 0.15 to 0.48% [35]–[39]. A total of 30 temperature sensors on neural probes were measured and the standard deviations of the temperature dependent resistance were shown as error bars. Two main factors contributed to these small fluctuations, including temperature stability of the water bath (±0.20 °C) and the accuracy of the commercial temperature sensor (±0.15 C). Overall, the temperature sensors showed an accuracy level of ±0.25 °C and a response time of 1.3 s.

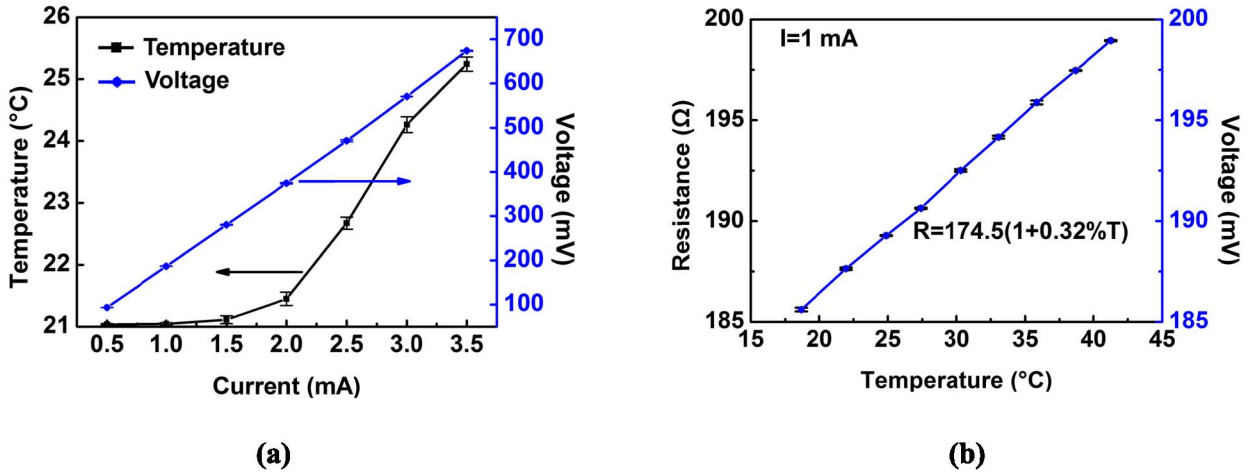

Fig. 4. (a) Temperature and voltage changes of temperature sensors as DC current was applied. (b) Resistance and voltage changes of resistive sensor as function of temperature showing good linearity and temperature coefficient of 0.32%.

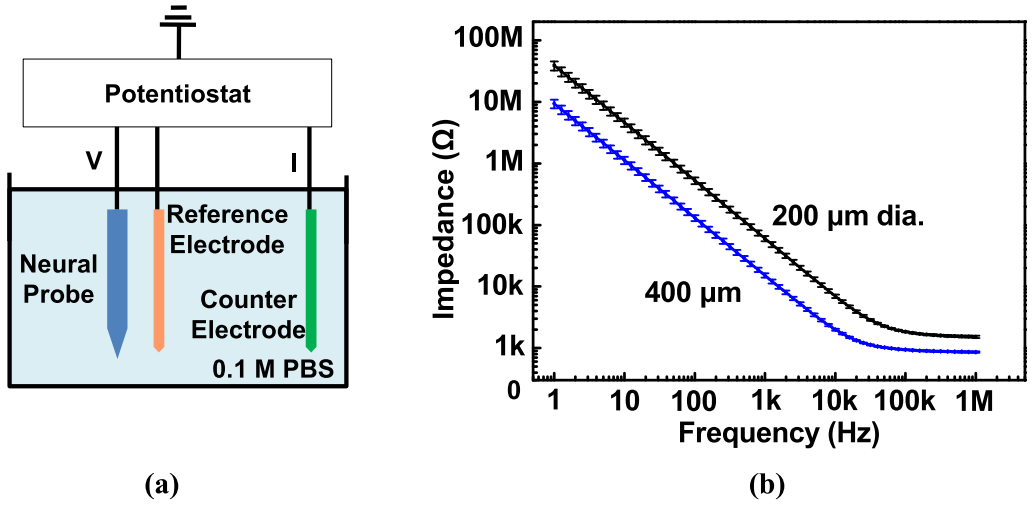

Fig. 5. (a) Impedance measurements of electrodes on neural probe in 0.1 M phosphate buffered saline (PBS) solution. (b) Impedance for 200 and 400 μm dia. electrodes as frequency varied from 1 Hz to 1MHz.

Each temperature sensor on the neural probe was calibrated before the probe was implanted to ensure the measured temperature was accurate. These resistive sensors were covered by 1 μm thick PI and the Au wires did not contact any of the tissues during *in vivo* measurements. In addition, the equipment and parameters for *in vivo* temperature measurement were identical to the ones used during calibration. All these resulted in reliable *in vivo* temperature measurements independent of the surrounding tissue and in accordance with the calibration results.

B. Characterization of Electrodes

There are mainly three important parameters to characterize electrodes for neural stimulation, including impedance, charge delivery capacity (CDC), and safe current limit. For impedance measurement, a potentiostat (Gamry 600, Gamry Instruments, USA) was used to supply the voltage. As shown in figure 5(a), the neural probe was immersed in 0.1 M PBS solution. The Pt counter electrode and Ag wire coated with AgCl reference electrode were also immersed in the PBS solution and connected to the potentiostat. A sinusoidal signal of 100 mV root mean square (rms) voltage with frequency ranging from 1 Hz to 1 MHz was applied to the electrodes of the neural probes and the corresponding current was collected in the Pt counter electrode. The impedance of the electrodes as a function of frequency is shown in figure 5(b). The results showed that impedance decreased with frequency and electrode size. Impedances for 200 and 400 μm dia. electrodes were 56.8 and 14.1 kΩ at 1 kHz, respectively.

Cyclic voltammetry (CV) measurement was used to obtain the charge delivery capacity (CDC) of the electrodes. The measurement system was the same as the impedance measurement system described previously. The potentiostat supplied a voltage ramped at 50 mV/s to the electrodes on the neural probe and a current was collected by the Pt counter electrode. The current-voltage traces are shown in figure 6. The safe charge injection window of 200 and 400 μm dia. electrodes was -0.21 to 0.42 V. Charge capacity for

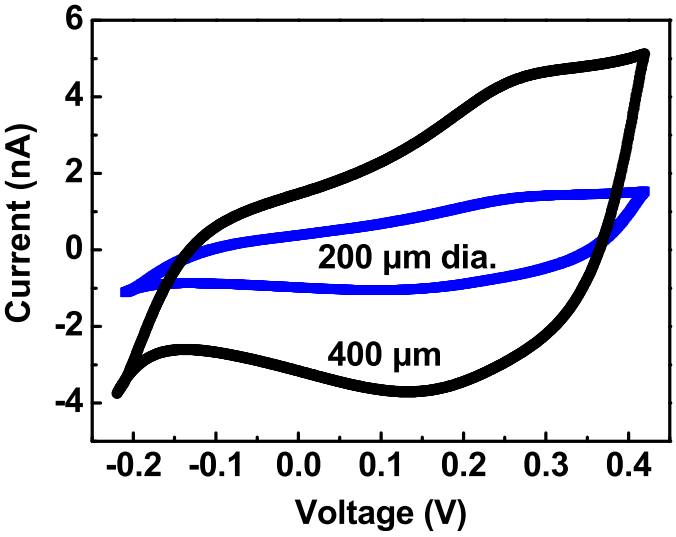

Fig. 6. Cyclic voltammetry (CV) for 200 and 400 μm dia. electrodes with safe charge injection window of −0.21 to 0.42 V.

200 and 400 μm dia. electrodes were calculated to be 17.14 and 60.83 nC, respectively.

Potential transient measurement (PTM) was used to determine the safe current limit of the electrode within the safe charge injection window. Neural probe and reference electrode were connected to a stimulus generator which provided bipolar rectangular current pulses to the electrodes on the neural probe. Safe current limit of an electrode was obtained by applying the current pulses in steps of 0.5 μA until the voltage between the electrodes on the neural probe and the reference electrode reached the threshold of the safe charge injection window of −0.21 V in the CV measurements. Safe current limit for 200 and 400 μm dia. electrodes were 8 and 13 μA, respectively.

C. Temperature Changes During Neural Probe Implantation in Retina and Brain

During *in vivo* testing, as neural probe is implanted, it is desirable to detect the position of the probe in the tissue. Electrode impedance has been used to measure neural probe position [40]–[43]. Since electrodes were in direct contact with the tissue, the electrode impedance could change due to exposure to the tissue. Temperature sensors used in this study were covered by a layer of PI film and had the advantage of not exposing the resistive sensors directly to the tissue, and hence the temperature measurements were more stable than impedance measurement to infer the position of the neural probes.

For the retinal implantation, neural probe was inserted from the incision near the limbus onto the retinal surface. A typical temperature variation measured by the temperature sensor on a neural probe during implantation in the retina is shown in figure 7(a). The temperature measurements were first taken in air with a stationery probe before insertion into the retina. Several pauses were made manually during the implantation to monitor temperature changes as the neural probe was moved towards the retina. Once the probe contacted the retina, the temperature became stable, and there was no further probe movement. A total of 9 neural probes were implanted and similar temperature responses were obtained.

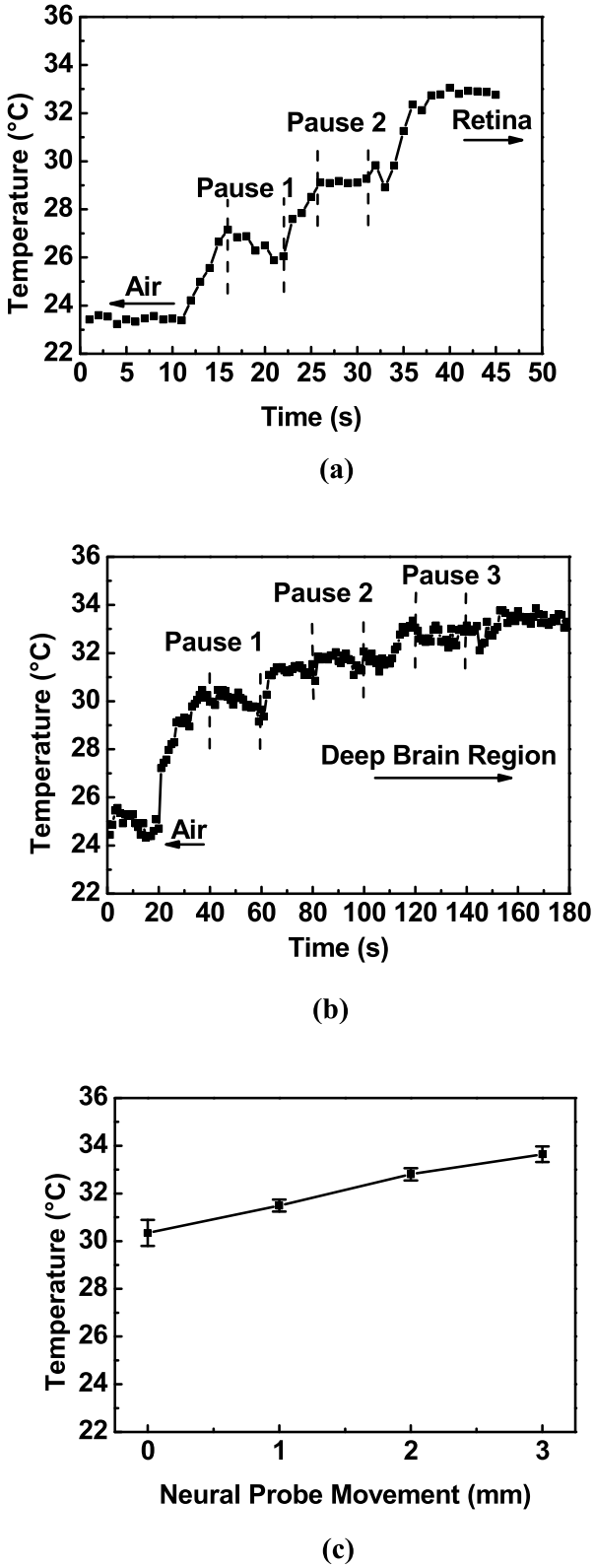

Fig. 7. (a) Temperature changes during insertion in retina with several pauses. (b) Temperature changes during insertion in brain with several pauses. (c) Temperature changes as neural probes were moved 3 mm from dura mater to deep brain region.

For the brain implantation, neural probe was implanted in the deep brain region of the anesthetized rat. The cortex of the rat remained exposed during measurements. Temperature measurements were taken using the temperature sensor on the neural probe while it was stationery in air. The probe was inserted manually by turning the stereotaxic apparatus through the brain surface and finally reached the deep brain region. A few pauses in different depths of 1 mm intervals were made during the neural probe implantation so that the probe was about 3 mm below the surface after the third pause. The temperature of the neural probe changed gradually from 24 to 34 °C, as shown in figure 7(b).

Three neural probes that were 2.5 cm long, 0.8 mm wide, and 116 μ m thick were each implanted into the brain of three different rats. Each probe was inserted from the surface (x = 0 mm) to the deep brain region (x = 3 mm). The relation between the depth of the neural probe in the brain and the average temperature change is shown in figure 7(c). As each neural probe travelled a total distance of 3 mm from the dura mater, the average temperature changed from 30.3 to 33.6 °C. The error bars in the figure represented deviation of each temperature measurement to the average temperature. The results showed that the temperature sensors on the neural probes were effective in monitoring the implantation process and the probe position.

D. In Vivo Temperature Changes During Stimulation in Retina and Brain

Electrical stimulation by applying current to the electrodes on neural probes could produce Joule heating and cause increase of temperature. During *in vivo* stimulation experiments, the charge balanced biphasic stimulation currents as shown in figure 3(c) were supplied. Two current levels were used for retina and brain stimulations. Low stimulation level was within the safe current limit of 8 and 13 μA for 200 and 400 μm dia. electrodes, respectively. High stimulation level was beyond the safe current limit with 100 and 200 μA for 200 and 400 μm dia. electrodes, respectively.

Each stimulation experiment took 30 min, including 10 min without stimulation, 10 min stimulation, followed by another 10 min without stimulation. The temperature was recorded every 1 s and averaged over 30 s. Figure 8(a) shows temperature changes of the retina during stimulation with two different stimulation levels. Under safe current limit of 8 μA each for the two 200 μm dia. electrodes and 13 μA each for the two 400 μm dia. electrodes, the temperature in the retina remained unchanged. When the stimulation current was increased beyond the safe current limit to 100 μA each for the two 200 μm dia. electrodes and 200 μA each for the two 400 μm dia. electrodes, the temperature of the retina gradually increased and a maximum temperature increase of 1.2 °C was recorded as shown in figure 8(b). After 10 min stimulation, the stimulation current was removed and the temperature of the retina started to decrease.

Similar stimulation experiments were carried out in deep brain region. The effects were nearly the same as stimulation in the retina. There was no temperature increase in the deep brain region under safe current limit of 8 μA each for the two 200 μm dia. electrodes and 13 μA each for the two 400 μm dia. electrodes as shown in figure 8(c). A maximum temperature increase of 1 °C was measured when stimulation current beyond the safe current limit of 100 μA each for two 200 μm dia. electrodes and 200 μA each for two 400 μm dia. electrodes was applied, as shown in figure 8(d). The results were comparable to the brain stimulation results of 0.3 to 0.8 °C temperature increase in previous studies [19], [44].

Stimulations in the retina and the deep brain region were repeated several times. A total of 6 rats were used for the *in vivo* experiments. The temperature changes due to the low and high levels retinal stimulations were obtained from 9 different eyes, each time with a fresh neural probe implanted. For the brain implantation, 3 neural probes were inserted into 3 different rats. Temperature changes due to 10 min stimulations in the retina and the brain at two different current levels are shown in figure 8(e). At the low stimulation current level with 8 and 13 μA each on the two 200 and 400 μm dia. electrodes, respectively, the average temperature change was 0.07 °C for the retina and −0.04 °C for the brain. With higher stimulation current level with 100 and 200 μA each on the two 200 and 400 μm dia. electrodes, respectively, the average temperature change was 0.82 °C for the retina and 0.74 °C for the brain. The standard deviations for the temperature changes were ±0.16 and ±0.23 °C, respectively, for retinal stimulations at the low and high stimulation levels, and ±0.14 and ±0.21 °C, respectively, for brain stimulations at the low and high stimulation levels.

IV. Discussion

Temperature increase induced by electrical stimulation using neural probes should be limited. For future generation of retinal neural probes with at least 1000 electrodes, stimulation current and electronic components on the probes could generate a lot of heat [8]. Likewise, large stimulation current used in deep brain stimulator (DBS) could cause excessive tissue heating and brain damage [45]. For epi-retinal prostheses application, the electrode charge density is possible to momentarily exceed the safe charge-injection limit due to the uneven electrode-retina distance, leading to thermal elevation in the eye. Charge density levels above the safe charge-injection limit were necessary to obtain perceptual threshold. In two human subjects implanted with 520 μm electrodes, the highest threshold obtained were 404 and 902 μA (0.58 and 1.3 mC/cm^2, respectively) while the safe charge-injection limit for the Pt electrode was 0.35 mC/cm^2 [30]. The reasons could be uneven electrode-retina distance, which leads to high threshold requirement for electrodes further away from the tack (to position the electrode array on the retina), or the heterogeneous degeneration of retinal neurons in the retina. Thus, it is necessary to monitor the temperature changes to infer the positions of the neural probes when they are implanted for stimulation.

Only the tip of the neural probe was immersed in the temperature controlled water bath to ensure that the calibration setup was similar to the *in vivo* measurements. Air above the

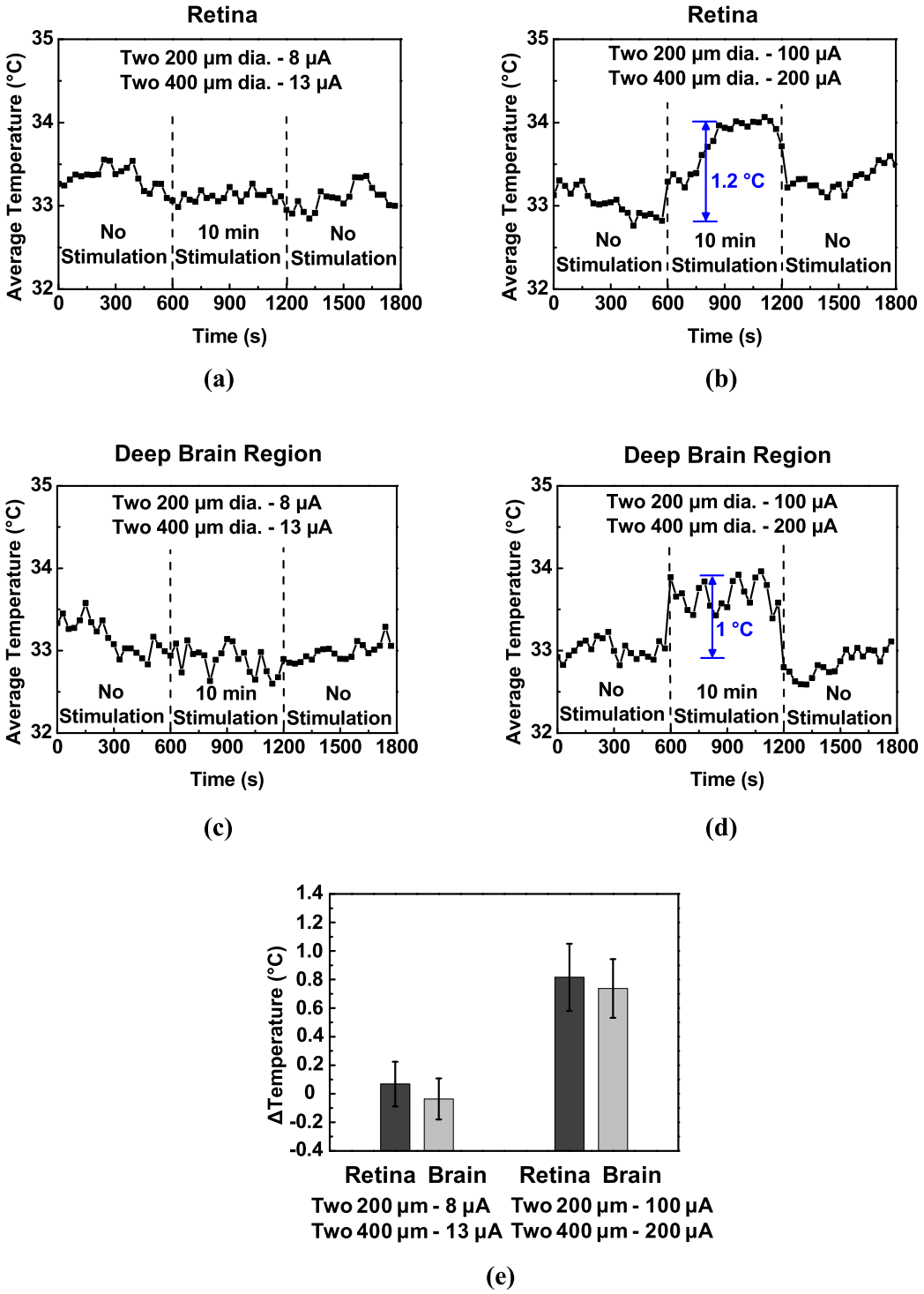

Fig. 8. Temperature changes during stimulation in retina under (a) safe current limit of 8 μA each for two 200 μm dia. electrodes and 13 μA each for two 400 μm dia. electrodes for 10 min and (b) beyond safe current limit of 100 μA each for two 200 μm dia. electrodes and 200 μA each for two 400 μm dia. electrodes for 10 min. Temperature changes during stimulation in deep brain region (c) under safe current limit of 8 μA each for two 200 μm dia. electrodes and 13 μA each for two 400 μm dia. electrodes for 10 min and (d) beyond safe current limit of 100 μA each for two 200 μm dia. electrodes and 200 μA each for two 400 μm dia. electrodes for 10 min. (e) Variations of temperature changes for retinal and brain stimulations under low and high levels stimulation current.

dura mater could influence the temperature measurement and this influence was minimized by decreasing the resistance of the interconnection wires, which were exposed in air. This was achieved by having 5 μm wide wires for the temperature sensors with a resistance of 190 Ω, while having 200 μm wide wires for the interconnections with a resistance of 10 Ω. The Au temperature sensors were covered by 1 μm thick PI to protect the sensor from direct contact with the surrounding tissue. Since the thermal conductivity of PI is 0.2 W/(m-k) and the PI thickness is 1 μm, it is expected that the

temperature sensors could detect the surrounding tissue temperature accurately through the PI cover, while preventing degradation of the Au resistors. Therefore, PI has been used frequently as an insulating layer in temperature sensors [35], [36], [38]. As shown in figures 8(a) and (c), there were no temperature changes when all four electrodes were stimulated at current levels below their safe limits. It would be useful to improve the safe limits of the neural probes and apply these temperature sensors to detect temperature changes at multiple current intensities below safe limits.

A total of 29 retinal stimulation experiments were made with low and high levels of stimulation. For stimulation in the retina, at low stimulation current with 8 μA each on the two 200 μm dia. electrodes and 13 μA each on the two 400 μm dia. electrodes, the average temperature rise was 0.07 °C with a standard deviation of 0.16 °C. Using higher level of stimulation current with 100 μA each on the two 200 μm dia. electrodes and 200 μA each on the two 400 μm dia. electrodes, the average temperature rise in the retina was 0.82 °C with a standard deviation of 0.23 °C. For stimulation in the brain, 3 and 4 experiments were carried out at the low and high level of stimulation current, respectively. As shown in figure 8(e), a similar trend of having a non-detectable temperature rise at low level of stimulation and a larger temperature increase at higher level of stimulation was observed.

Temperature increase could be due to many factors during stimulation. The heat balance during stimulation could be described as [46]:

$$C\rho\frac{\partial T}{\partial t} = \nabla\cdot(K\nabla T) + A_{\mathrm{o}} - B_{\mathrm{o}}(T - T_{\mathrm{B}}) + \rho SAR + P_{\mathrm{Density}} + P_{\mathrm{Electronics}} \quad (2)$$

where T is temperature (°C), C is specific heat (J/ (kg-°C)), ρ is tissue density (kg/m^3), K is thermal conductivity of tissue (J/(m-s-°C)), A_{o} is basic metabolic rate (J/(m^3-s)), B_{o} is blood perfusion coefficient (J/(m-s-°C)), T_{B} is temperature of blood (°C), *SAR* is a measure of absorbed power per unit mass of tissue due to exposure to electromagnetic fields (W/kg), P_{Density} is the power dissipated by the implanted electrode array (W/m^3), and $P_{\mathrm{Electronics}}$ is the power dissipated by the implanted electrical circuit (W/m^3). In the present experimental setup, $P_{\mathrm{Electronics}}$ mainly included the self-heating of the temperature sensor due to the 1 mA DC current applied and the temperature increase induced by the stimulation current through the Au interconnecting wires and the electrodes. Temperature increased by self-heating of the resistive sensor was <0.05 °C. Since the Au interconnecting wires and the electrodes had much lower resistance compared to the surrounding tissue, heating induced by the stimulation current therefore would be mainly related to heating of the tissue around the electrodes. In our experiment, *SAR* and $P_{\mathrm{Electronics}}$ could be neglected and equation (2) is simplified:

$$C\rho\frac{\partial T}{\partial t} = \nabla\cdot(K\nabla T) + A_{\mathrm{o}} - B_{\mathrm{o}}(T - T_{\mathrm{B}}) + P_{\mathrm{Density}} \quad (3)$$

For the *in vivo* measurements, the room temperature was 22 °C and the humidity was 60-70%. The body temperature of the rat was maintained at physiological range (35.8-37.5 °C) by a heating pad. The changes of temperature recorded in eye and brain were a little bit lower than body temperature, while still kept in normal level and quite similar in other published data [21], [47].

Besides temperature changes due to stimulation current applied on the electrodes, there were several factors that could also influence temperature including air temperature variations, body and blood temperature variations [10], as well as metabolic responses and blood perfusion [11], [44]. FEM simulations and experimental results showed 2 °C temperature increase due to electronic components on the neural probe if there were no metabolic responses or blood perfusion [20], [48]. We observed that the body temperature of rats would decrease from 35 to 30 °C in 30 min after death even with the heating pad since there was no blood perfusion to regulate the body temperature. Our work to measure temperature changes in the retina of the eye and in the deep brain region induced by stimulation current as shown in figure 8 were the first demonstration of using integrated temperature sensors in neural probes to monitor temperature increase during electrical stimulation with active metabolic responses and blood perfusion. At the higher level stimulation current, the rise time for the increased temperature could vary from 10 to 200 s, much slower than the rise time of 1.3 s for the temperature sensor. The rise time variations due to electrical stimulation were partly due to the differences in physiological responses for various rats. Typically, stimulation induced temperature increase has a faster rise time in the deep brain region compared to the retina. This could be due to the vitreous body which acts as a heat sink next to the retina that has different heat capacity or conductivity compared to the brain tissue.

V. Conclusion

Flexible PI-based neural probes integrated with Au temperature sensors were developed to monitor the temperature changes during implantation and stimulation in the retina of the eye and the deep brain region. The Au temperature sensor had a good linearity and the temperature coefficient of the temperature sensor was 0.32%. For neural probe implantation, temperature changed from air temperature to the body temperature gradually. The positions of the neural probe could be monitored by the temperature changes. Once the measured temperature became stable, the neural probe had reached the desired implantation location where the temperature was not affected by the environment. For electrical stimulation through the electrodes in the neural probes, high level stimulation current of 100 μA each for the two 200 μm dia. electrodes and 200 μA each for the two 400 μm dia. electrodes induced average temperature increase of 0.82 °C in the retina and 0.74 °C in the deep brain region. The integrated temperature sensors in the neural probes were useful to monitor the position of the implanted probes and to prevent thermal damage to the tissue.

Acknowledgment

The authors like to thank all the members of the Pang and Chan labs for their ideas, discussions, and encouragement.

REFERENCES

[1] J. M. Delgado and T. Hanai, "Intracerebral temperatures in free-moving cats," *Amer. J. Physiol.*, vol. 211, pp. 755–769, Sep. 1966.

[2] V. B. Brooks, "Study of brain function by local, reversible cooling," *Rev. Physiol., Biochem. Pharmacol.*, vol. 95, pp. 1–109, 1983.

[3] T. M. Seese, H. Harasaki, G. M. Saidel, and C. R. Davies, "Characterization of tissue morphology, angiogenesis, and temperature in the adaptive response of muscle tissue to chronic heating," *Lab. Invest., J. Tech. Methods Pathol.*, vol. 78, no. 12, pp. 1553–1562, 1998.

[4] E. A. Kiyatkin, P. L. Brown, and R. A. Wise, "Brain temperature fluctuation: A reflection of functional neural activation," *Eur. J. Neurosci.*, vol. 16, no. 1, pp. 164–168, 2002.

[5] K. Okabe, N. Inada, C. Gota, Y. Harada, T. Funatsu, and S. Uchiyama, "Intracellular temperature mapping with a fluorescent polymeric thermometer and fluorescence lifetime imaging microscopy," *Nature Commun.*, vol. 3, Feb. 2012, Art. no. 705.

[6] K. Shibasaki, M. Suzuki, A. Mizuno, and M. Tominaga, "Effects of body temperature on neural activity in the hippocampus: Regulation of resting membrane potentials by transient receptor potential vanilloid 4," *J. Neurosci.*, vol. 27, no. 7, pp. 1566–1575, 2007.

[7] C. Paviolo, A. C. Thompson, J. Yong, W. G. A. Brown, and P. R. Stoddart, "Nanoparticle-enhanced infrared neural stimulation," *J. Neural Eng.*, vol. 11, no. 6, p. 065002, 2014.

[8] K. Mathieson *et al.*, "Photovoltaic retinal prosthesis with high pixel density," *Nature Photon.*, vol. 6, pp. 391–397, Nov. 2012.

[9] N. L. Opie *et al.*, "Retinal prosthesis safety: Alterations in microglia morphology due to thermal damage and retinal implant contact," *Invest. Ophthalmol. Vis. Sci.*, vol. 53, pp. 7802–7812, Nov. 2012.

[10] E. Y. K. Ng and E. H. Ooi, "FEM simulation of the eye structure with bioheat analysis," *Comput. Methods Programs Biomed.*, vol. 82, no. 3, pp. 268–276, 2006.

[11] K. C. Gokul, D. B. Gurung, and P. R. Adhikary, "Effect of blood perfusion and metabolism in temperature distribution in human eye," *Adv. Appl. Math. Biosci.*, vol. 4, no. 1, pp. 13–23, 2013.

[12] A. Narasimhan and K. K. Jha, "Bio-heat transfer simulation of retinal laser irradiation," *Int. J. Numer. Methods Biomed. Eng.*, vol. 28, no. 5, pp. 547–559, 2012.

[13] C. Buccella, V. D. Santis, and M. Feliziani, "Prediction of temperature increase in human eyes due to RF sources," *IEEE Trans. Electromagn. Compat.*, vol. 49, no. 4, pp. 825–833, Nov. 2007.

[14] A. Hirata, "Temperature increase in human eyes due to near-field and far-field exposures at 900 MHz, 1.5 GHz, and 1.9 GHz," *IEEE Trans. Electromagn. Compat.*, vol. 47, no. 1, pp. 68–76, Feb. 2005.

[15] S. Kim, P. Tathireddy, R. A. Normann, and F. Solzbacher, "Thermal impact of an active 3-D microelectrode array implanted in the brain," *IEEE Trans. Neural Syst. Rehabil. Eng.*, vol. 15, no. 4, pp. 493–501, Dec. 2007.

[16] J. Kandulla, H. Elsner, R. Birngruber, and R. Brinkmann, "Noninvasive optoacoustic online retinal temperature determination during continuous-wave laser irradiation," *J. Biomed. Opt.*, vol. 11, no. 4, pp. 041111-1–041111-13, 2006.

[17] S. Koinzer *et al.*, "Temperature-controlled retinal photocoagulation—A step toward automated laser treatment," *Invest. Ophthalmol. Vis. Sci.*, vol. 53, pp. 3605–3614, Jun. 2012.

[18] C. Wang *et al.*, "Determining intracellular temperature at single-cell level by a novel thermocouple method," *Cell Res.*, vol. 21, pp. 1517–1519, Jul. 2011.

[19] M. M. Elwassif, A. Datta, A. Rahman, and M. Bikson, "Temperature control at DBS electrodes using a heat sink: Experimentally validated FEM model of DBS lead architecture," *J. Neural Eng.*, vol. 9, no. 4, p. 046009, 2012.

[20] N. L. Opie, A. N. Burkitt, H. Meffin, and D. B. Grayden, "Heating of the eye by a retinal prosthesis: Modeling, cadaver and *in vivo* study," *IEEE Trans. Biomed. Eng.*, vol. 59, no. 2, pp. 339–345, Feb. 2012.

[21] Z. Yu, K. Schulmeister, N. Talebizadeh, M. Kronschläger, and P. G. Söderberg, "Ocular temperature elevation induced by threshold *in vivo* exposure to 1090-nm infrared radiation and associated heat diffusion," *J. Biomed. Opt.*, vol. 19, no. 10, p. 105008, 2014.

[22] H. Sun, N. Hosszufalusi, E. R. Mikula, and T. Juhasz, "Simulation of the temperature increase in human cadaver retina during direct illumination by 150-kHz femtosecond laser pulses," *J. Biomed. Opt.*, vol. 16, no. 10, p. 108001, 2011.

[23] A. C. Thompson, S. A. Wade, P. J. Cadusch, W. G. A. Brown, and P. R. Stoddart, "Modeling of the temporal effects of heating during infrared neural stimulation," *J. Biomed. Opt.*, vol. 18, no. 3, p. 035004, 2013.

[24] A. N. Smith, M. P. Christian, S. L. Firebaugh, G. W. Cooper, and B. G. Jamieson, "Predicting and managing heat dissipation from a neural probe," *Biomed. Microdevices*, vol. 17, p. 81, Aug. 2015.

[25] M. Zhu, J. J. H. Ackerman, A. L. Sukstanskii, and D. A. Yablonskiy, "How the body controls brain temperature: The temperature shielding effect of cerebral blood flow," *J. Appl. Physiol.*, vol. 101, no. 5, pp. 1481–1488, 2006.

[26] P. J. Rousche, D. S. Pellinen, D. P. Pivin, J. C. Williams, R. J. Vetter, and D. R. Kipke, "Flexible polyimide-based intracortical electrode arrays with bioactive capability," *IEEE Trans. Biomed. Eng.*, vol. 48, no. 3, pp. 361–371, Mar. 2001.

[27] G. K. Lott, III, and R. R. Hoy, "A polyimide pressure-contact multielectrode array for implantation along a submillimeter neural process in small animals," *IEEE Trans. Biomed. Eng.*, vol. 55, no. 6, pp. 1728–1732, Jun. 2008.

[28] S. R. I. Gabran *et al.*, "3-D flexible nano-textured high-density microelectrode arrays for high-performance neuro-monitoring and neurostimulation," *IEEE Trans. Neural Syst. Rehabil. Eng.*, vol. 22, no. 5, pp. 1072–1082, Sep. 2014.

[29] S. H. Kim, S. H. Cho, N.-E. Lee, H. M. Kim, Y. W. Nam, and Y.-H. Kim, "Adhesion properties of Cu/Cr films on polyimide substrate treated by dielectric barrier discharge plasma," *Surf. Coat. Technol.*, vol. 193, pp. 101–106, Apr. 2005.

[30] C. de Balthasar *et al.*, "Factors affecting perceptual thresholds in epiretinal prostheses," *Invest. Ophthalmol. Vis. Sci.*, vol. 49, pp. 2303–2314, Jun. 2008.

[31] A. K. Ahuja *et al.*, "Factors affecting perceptual threshold in Argus II retinal prosthesis subjects," *Transl. Vis. Sci. Technol.*, vol. 2, p. 1, Apr. 2013.

[32] M. S. Humayun *et al.*, "Pattern electrical stimulation of the human retina," *Vis. Res.*, vol. 39, no. 15, pp. 2569–2576, 1999.

[33] C. Sekirnjak, P. Hottowy, A. Sher, W. Dabrowski, A. M. Litke, and E. J. Chichilnisky, "Electrical stimulation of mammalian retinal ganglion cells with multielectrode arrays," *J. Neurophysiol.*, vol. 95, no. 6, pp. 3311–3327, 2006.

[34] M. Abramian, N. H. Lovell, J. W. Morley, G. J. Suaning, and S. Dokos, "Activation of retinal ganglion cells following epiretinal electrical stimulation with hexagonally arranged bipolar electrodes," *J. Neural Eng.*, vol. 8, no. 3, p. 035004, 2011.

[35] Y. Moser and M. A. M. Gijs, "Miniaturized flexible temperature sensor," *J. Microelectromech. Syst.*, vol. 16, no. 6, pp. 1349–1354, Dec. 2007.

[36] S. Y. Xiao, L. F. Che, X. X. Li, and Y. L. Wang, "A novel fabrication process of MEMS devices on polyimide flexible substrates," *Microelectron. Eng.*, vol. 85, no. 2, pp. 452–457, Feb. 2008.

[37] C. Li *et al.*, "Brain temperature measurement: A study of *in vitro* accuracy and stability of smart catheter temperature sensors," *Biomed. Microdevices*, vol. 14, no. 1, pp. 109–118, 2012.

[38] C.-Y. Liu *et al.*, "*In vivo* thermal evaluation of a subretinal prosthesis using an integrated resistance temperature detector," *J. Micro/Nanolithogr., MEMS, MOEMS*, vol. 13, no. 1, p. 013006, 2014.

[39] Z. Yang, Y. Zhang, T. Itoh, and R. Maeda, "Flexible implantable microtemperature sensor fabricated on polymer capillary by programmable UV lithography with multilayer alignment for biomedical applications," *J. Microelectromech. Syst.*, vol. 23, no. 1, pp. 21–29, Feb. 2014.

[40] L. Johnson *et al.*, "Impedance-based retinal contact imaging as an aid for the placement of high resolution epiretinal prostheses," *J. Neural Eng.*, vol. 4, no. 1, pp. S17–S23, 2007.

[41] A. Ray, L. L.-H. Chan, A. Gonzalez, M. S. Humayun, and J. D. Weiland, "Impedance as a method to sense proximity at the electrode-retina interface," *IEEE Trans. Neural Syst. Rehabil. Eng.*, vol. 19, no. 6, pp. 696–699, Dec. 2011.

[42] T. Torfs *et al.*, "Two-dimensional multi-channel neural probes with electronic depth control," *IEEE Trans. Biomed. Circuits Syst.*, vol. 5, no. 5, pp. 403–412, Oct. 2011.

[43] J. A. Majdi, S. Minnikanti, N. Peixoto, A. Agrawal, and E. D. Cohen, "Access resistance of stimulation electrodes as a function of electrode proximity to the retina," *J. Neural Eng.*, vol. 12, no. 1, p. 016006, 2015.

[44] M. M. Elwassif, Q. Kong, M. Vazquez, and M. Bikson, "Bio-heat transfer model of deep brain stimulation-induced temperature changes," *J. Neural Eng.*, vol. 3, no. 4, pp. 306–315, 2006.
[45] J. C. LaManna, K. A. McCracken, M. Patil, and O. J. Prohaska, "Stimulus-activated changes in brain tissue temperature in the anesthetized rat," *Metabolic Brain Disease*, vol. 4, no. 4, pp. 225–237, 1989.
[46] G. Lazzi, "Thermal effects of bioimplants," *IEEE Eng. Med. Biol. Mag.*, vol. 24, no. 5, pp. 75–81, Sep. 2005.
[47] M. Zhu, J. J. H. Ackerman, and D. A. Yablonskiy, "Body and brain temperature coupling: The critical role of cerebral blood flow," *J. Comparative Physiol. B*, vol. 179, no. 6, pp. 701–710, 2009.
[48] H. Sailer *et al.*, "Investigation of thermal effects of infrared lasers on the rabbit retina: A study in the course of development of an active subretinal prosthesis," *Graefe's Arch. Clin. Experim. Ophthalmol.*, vol. 245, no. 8, pp. 1169–1178, 2007.

Jiaqi Wang was born in Dalian, China. He received the B.S. and M.S. degrees from the Department of electronics engineering from Shenyang University of Technology, Shenyang, China, in 2003 and 2006, respectively, and the Ph.D. degree from the Department of Electronic Engineering, Dalian University of Technology, Dalian, in 2010. He was with the Dalian Institute of Semiconductor Technology and the School of Electronic Science and Technology, Dalian University of Technology. From 2014 to 2016, he was the Hong Kong Scholar with the Department of Electronic Engineering, City University of Hong Kong, Hong Kong, China.

He is currently with the School of Microelectronics, Dalian University of Technology. His research interests include micromachining technology for biomedical application and integrated sensor system on chip.

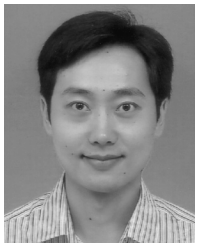

Hui Xie received the M.D degree in clinical medicine from the Nanhua University School of Medicine, China, and the Ph.D. degree in neuroscience from The Chinese University of Hong Kong, Hong Kong. He is currently a Research Fellow with the Center for Biosystems, Neuroscience, and Nanotechnology, City University of Hong Kong. His research interests include the pathogenesis and treatment of neurodegenerative disorders, neuron plasticity, and analysis of neural signals.

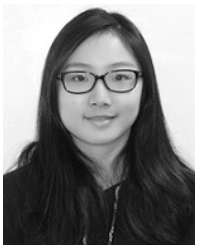

Tsing Chung received the B.Eng. and M.Phil. degrees in electronic engineering from the City University of Hong Kong. Her research interests include microfabrication technology for neural probes for detection of neural signals.

Leanne Lai Hang Chan received the B.Eng. degree in electrical and electronic engineering from the University of Hong Kong, and the M.S. degree in electrical engineering and the Ph.D. degree in biomedical engineering from the University of Southern California. She is currently an Assistant Professor with the Department of Electronic Engineering, City University of Hong Kong. Her research interests include artificial vision, retinal prosthesis, and neural recording.

Stella W. Pang (F'99) received the B.Sc. degree from Brown University, Providence, RI, USA, in 1977, the M.Sc. and the Ph.D. degrees from Princeton University, Princeton, NJ, USA, in 1978 and 1981, respectively.

From 1981 to 1989, she was with the Lincoln Laboratory, Massachusetts Institute of Technology, Lexington, MA, USA. She served as the Associate Dean for Graduate Education and International Programs with the College of Engineering from 2002 to 2007. She was a Professor of Electrical Engineering and Computer Science with the University of Michigan, Ann Arbor, MI, USA, from 1990 to 2011. She joined the City University of Hong Kong as the Chair Professor with the Department of Electronic Engineering in 2012. She is currently the Department Head and the Director of the Center for Biosystems, Neuroscience, and Nanotechnology. She has over 400 technical papers, book chapters, and invited presentations and is the editor and author of 16 books, journals and conference proceedings. Her research interests include nanofabrication technology for microelectromechanical, biomedical, microelectronic, and optical devices.

She holds nine patents granted in nanotechnology and microsystems. She is a fellow of the Electrochemical Society and the American Vacuum Society.